Draft version October 17, 2022
Typeset using LaTeX default style in AASTeX631

Radio Astronomy: Data Collection

Savannah Gramze,[1] Makennah Bristow,[1] Maria Galloway-Sprietsma,[1] and Natalia Guerrero[1]

[1] *University of Florida, Gainesville, FL 32611 USA*

1. BACKGROUND

Radio astronomy is the science of learning about the universe through observations of electromagnetic radiation in the radio part of the spectrum. Instead of reflective mirrors or lenses, we use metal dishes painted with special reflective coatings to collect radio light. The purpose of this lab is to learn about radio astronomy, and its similarities and differences to other forms of astronomy.

Instead of light pollution from the lights from cities, the Moon or Sun limiting the eyesight of radio telescopes, radio frequency interference (RFI) from technology overwhelms the radio light from space. Luckily, RFI can be accounted for and removed by knowing the common sources, such as satellites, and preparing for them.

The most common element in the universe is Hydrogen, with the most common molecule being H_2. We primarily observe Hydrogen in the radio with the 21 cm line. The 21 cm line is due to an electron belonging to neutral Hydrogen undergoing a spin flip transition. Because of the great abundance of Hydrogen in the universe, we can use this transition to map out the Milky Way and its spiral arms.

2. METHODOLOGY

The first step to understanding radio astronomy is to understand the equipment, so we took stock of the tools provided: a radio telescope, dipole antenna, RTL-SDR (RealTek Software-Defined Radio) USB (Universal Serial Bus) dongle, LNA (Low-Noise Amplifier), Coaxial Adapter (big to little), Coaxial Adapter (male-to-male, little-to-little), Coaxial cable, 50-ohm terminator, Observing laptop, Power cord for laptop, and USB extension cord. One of our phones, with an astronomy app installed, acted as a tool for measuring the altitude and azimuth of the telescope. We put together the telescope fully to ensure we understood how it all fit together.

We next set up the computer for taking observations, installing the required software and taking five one second scans and single one minute calibration scans per each type of calibration: resistor on, resistor off, LNA on with resistor, LNA on without resistor. We gave the `record_calibration` code a timeout of 3 seconds to keep it from throwing errors. For frequency calibration, we removed the LNA from the telescope's signal path and recorded the measured frequency offset: $-0.000\,325\,751\,32$ Hz. The purpose of this was to account for radio signal interference from NOAA weather services. To obtain calibrated data, we used a technique called frequency switching, where we record data at two frequencies separated by more than the expected line-width, but less than the receiver bandwidth, integrating for two consecutive observations and then taking the difference.

After taking our calibration scans, we moved outside to begin our observations. We took the antenna outside and set it up with the observation laptop. We first took an initial scan of the zenith to measure the base emission. We then pointed the antenna as at the Milky Way, aiming for the Galactic disk by approximating the location with an astronomy app on our phones. We measured the altitude and azimuth of the telescope by positioning a smartphone with an astronomy app at the tip of the dish. We used the `record_integration` code to take integrations of 1 minute each, keeping the dish still for three or four observations per pointing. We repeated observations at two other locations approximately pointed at the Galactic disk.

3. RESULTS

After recording the observations, we analyzed the resulting spectra for detections of the 21 cm line. The velocity redshift of the lines has not been corrected for the velocity of the Earth and Sun. As the observations were only integrated for one minute each to prevent integrating over larger swaths of sky, the signal to noise ratio is not the best for all possible detections of HI along the line of sight. Longer integrations that track the position on the sky would reveal better signal. Additionally, the frequencies of detected emission were all very similar, most likely due to the same relative motions of the detected gas.

We median combined the spectra for each pointing, and then subtracted the zenith integration to attempt to reduce the noise. We analyzed the spectra to identify the HI 21 cm line and its offset from $0\,\mathrm{km\,s^{-1}}$. The spectra are shown in Figure 3, and the velocity of the HI emission is shown in Table 5.

4. CONCLUSION

The goal of this lab was to learn how to use a radio telescope to observe the Milky Way Galaxy in radio light, specifically the HI 21 cm line. Our purpose was to observe emission from the Milky Way's spiral arms so that we could eventually use the measurements to create a map of the Galactic disk in radio emission. In Figure 3 are plotted the median combined and zenith subtracted spectra of each pointing. Pointing One and Pointing Three have similar spectra due to the observations being relatively close together in the sky. The velocities of the HI lines are presented in Table 5.

There is some uncertainty as to whether or not the 21 cm line was truly detected, as the identified peaks are low signal to noise, and RFI contaminated the spectra. Additionally, since the pointings were above the Galactic disk, little HI emission was included in the radio antenna's beam. In the future, longer exposures with better accuracy pointing at the Galactic disk are needed to measure the velocity of HI emission in our Galaxy. A radio antenna that tracks the sky would be optimal.

5. FIGURES AND TABLES

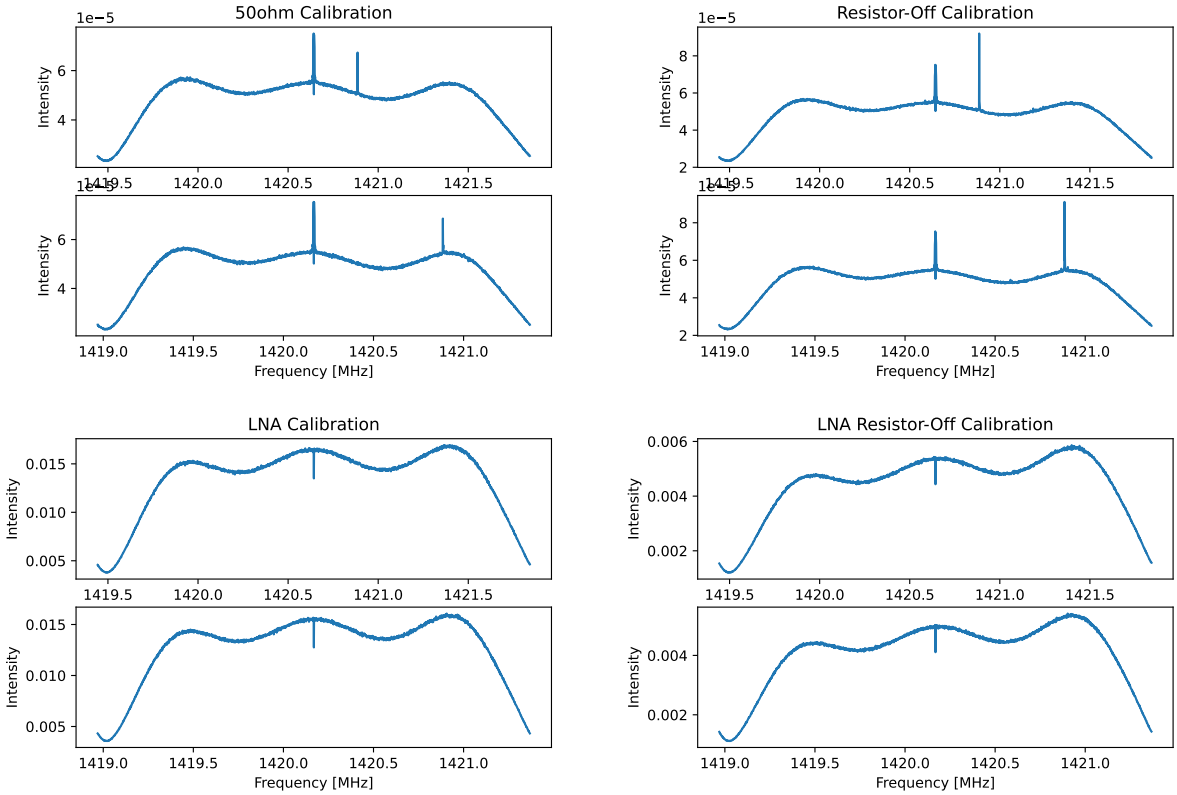

Figure 1. Spectra of the calibration scans taken (top left) with the 50 ohm resistor on, (top right) with the resistor off, (bottom left) with the resistor on and LNA on, and (bottom right) with the LNA on but resistor off. The top plots in each quadrant are of power1, and the bottom are power2. These plots show possible sources of RFI, and the state of the data before performing frequency switching.

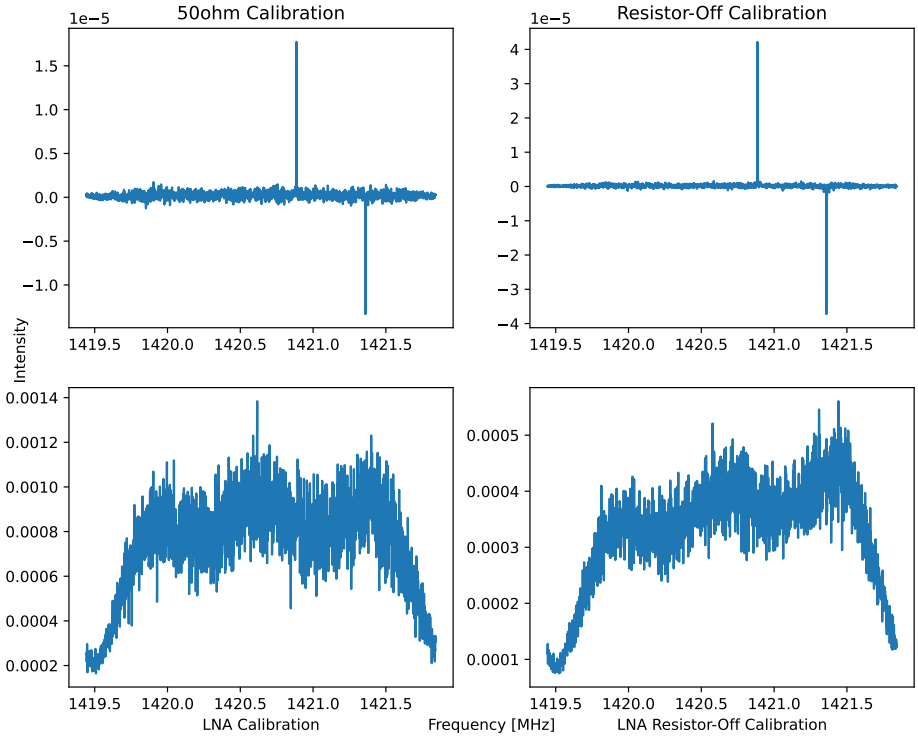

Figure 2. Four panel plot of the results of using frequency switching to calibrate data. The spikes on the top two plots are due to the Gainesville NOAA weather station, which are removed with the LNA.

Obs ID	Observation Time	Altitude °	Azimuth °	Gal. Longitude °	Gal. Latitude °	tint s	Notes
0	2022-09-22 19:12:00	125.8	87.5	41.2508	75.3654	60	Zenith
1	2022-09-22 19:22:32	128.8	66.6	18.1863	54.4328	60	Gal obs 1
2	2022-09-22 19:33:36	128.8	66.6	20.2293	52.031	60	Gal obs 1
3	2022-09-22 19:36:48	128.8	66.6	20.7876	51.3335	60	Gal obs 1
4	2022-09-22 19:40:24	128.8	66.6	21.40013	50.5465	60	Gal obs 1
5	2022-09-22 19:43:30	169.7	51.1	344.6783	44.7678	60	Gal obs 2
6	2022-09-22 19:46:45	169.7	51.1	345.5769	44.2800	60	Gal obs 2
7	2022-09-22 19:50:16	169.7	51.1	346.5308	43.7429	60	Gal obs 2
8	2022-09-22 19:55:30	112.9	66.3	32.4631	45.1346	60	Gal obs 3
9	2022-09-22 19:58:39	112.9	66.3	32.8247	44.43118	60	Gal obs 3
10	2022-09-22 20:02:00	112.9	66.3	33.2046	43.6830	60	Gal obs 3

Table 1. Observation Log, including the time of the observation, altitude and azimuth as recorded by smart phone app, and calculated Galactic longitude and latitude.

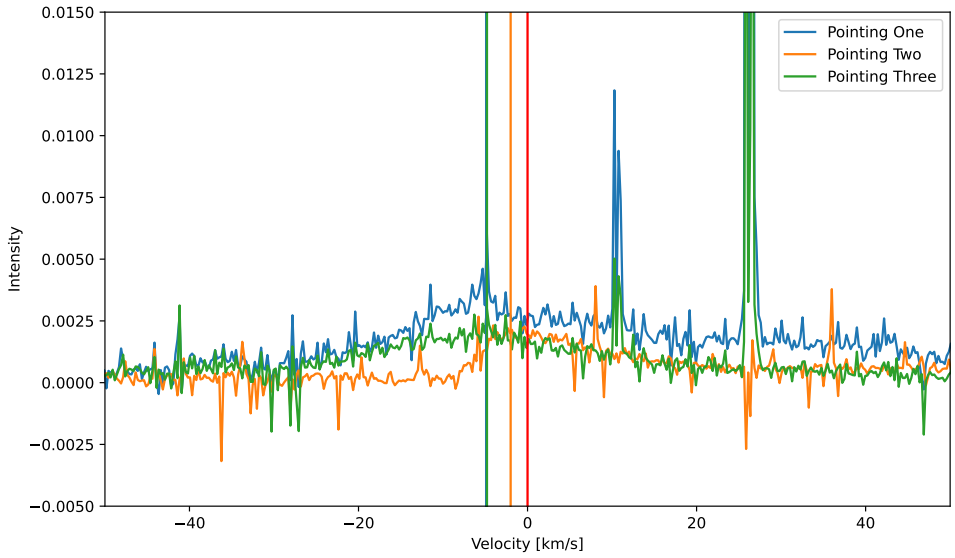

Figure 3. Spectra of the three pointings observed. The velocity has not been corrected for the motion of the Earth or Sun. The red vertical line marks 0 km s^{-1}, the rest frequency for the 21 cm line. The vertical lines corresponding to the legend colors for each pointing mark the peak velocity of the HI 21 cm line near 0 km s^{-1}. There are other, higher intensity lines, but we assume that any lines with narrow widths are noise or RFI. The Pointing One and Pointing Three lines are approximately at the same velocity.

Observation ID	Galactic Longitude °	Galactic Latitude °	Velocity Peak of HI km s^{-1}
0	41.25081715543127	75.36546495616105	0.0
1	18.186327724383414	54.432877569693325	-5.0
2	20.229303665428397	52.0315301058366	-5.0
3	20.787633312414393	51.333512553712715	-5.0
4	21.40013451624622	50.54652166205323	-5.0
5	344.67839760408486	44.767894553194004	-2.0
6	345.5769822027306	44.28009261870978	-2.0
7	346.53083642571374	43.74293275712039	-2.0
8	32.463100290995484	45.13467477505573	-4.8
9	32.82477848209726	44.431185766524926	-4.8
10	33.20465270121665	43.68302536139487	-4.8

Table 2. Table of observations